Is there a relation between glass-forming ability and first sharp diffraction peak?

1995 J. Phys.: Condens. Matter 7 3099

(http://iopscience.iop.org/0953-8984/7/16/006)

J. Phys.: Condens. Matter 7 (1995) 3099–3114. Printed in the UK

Is there a relation between glass-forming ability and first sharp diffraction peak?

E A Chechetkina

Institute of General and Inorganic Chemistry, Leninsky Prospect 31, Moscow 117907, Russia

Received 22 November 1995

Abstract. Available data for the first sharp diffraction peak (FSDP), which is observed in many amorphous substances including glasses, is analysed from the point of view of the glass-forming ability (GFA) of a substance. To clarify the subject, the ways of defining GFA and numerical evaluation are discussed first of all. It is shown that, in contrast to intuition, there is no direct connection between FSDP and GFA. Moreover, a non-glass-forming melt or a glass at the boundary of the glass-forming region may demonstrate strong and narrow FSDP. On the other hand, the obtained correlations between FSDP characteristics (position, intensity, halfwidth) and sample parameters, both internal (chemical composition, short-range order) and external (temperature, pressure), need explanations in terms of models that try to understand the origin of FSDP and corresponding medium-range order in the amorphous state, the glassy state being a particular case.

1. Introduction

The first sharp diffraction peak (FSDP) in the structure factor, a characteristic feature of glasses and glass-forming liquids, has attracted attention for a long time (see [1–4] for reviews). However, its understanding has remained controversial up to now. The only generally accepted statement concerning FSDP is that it is the signature of medium-range order (MRO) or, synonymously, intermediate-range order of about 10 Å scale beyond ordinary short-range order of 2–4 Å scale.

As far as FSDP is typical for glasses, one may conclude that the stronger it is, the higher the glass-forming ability (GFA) of a substance. In fact, in the excellent glass-former B_2O_3 the FSDP at $Q_1 \sim 1.5$ Å (a characteristic value for oxide glasses) is the strongest peak in the diffraction pattern (see e.g. [2]), while in the poor glass-former Sb_2S_3, which may be obtained only at fast cooling of a small amount of melt, there is a small but still obvious FSDP at $Q_1 \sim 1.0$ Å (characteristic of chalcogenide glasses) [5]. Moreover, when analysing the glass-forming system A_xB_{1-x} one may observe that FSDP vanishes at the boundaries of the glass-forming region (see examples in [1, 2]). This connection was specially investigated recently by Salmon and Liu [6] in a series of Ge_ySe_{1-y} melts with $y = 0.30$, 0.40, 0.50 and 1.00 (where the first is a glass-forming liquid, the intermediates are very poor glass-formers, and Ge is non-glass-forming at all, i.e. it cannot be obtained by melt cooling by ordinary quenching rates of $\sim 10^2$ K s^{-1}. It was shown that even in GeSe ($y = 0.50$) FSDP is virtually eliminated.

However, there is no direct connection between FSDP and GFA, because a strong characteristic FSDP is observed in the non-glass-forming melts APB [7] and ASn [8] (A = K, Na, Rb, Cs), which cannot be obtained in the solid amorphous state. On the other hand, it was shown recently [9] that these melts clearly differ from glass-forming ones when

0953-8984/95/163099+16$19.50

scaling their position Q_1 in the ξ–r_1 plot, where $\xi = d/r_1$ (with $d = 2\pi/Q_1$ known as 'equivalent distance') is the scale of MRO and r_1 is the first interatomic distance obtained from the radial distribution function. Each group (glasses, amorphous metals, APb melts, etc.) occupies a definite curve in the ξ–r_1 plot, but the concrete disposition of a glass on the 'glassy' correlation curve says nothing about the GFA of the corresponding substance in comparison with other glass-forming substances.

Thus, the connection between FSDP and GFA, if one does exist, is not trivial and needs special investigation by using both FSDP data (position, intensity, halfwidth) and GFA data, with special attention paid to the numerical characterization of GFA (see section 2). Such an analysis represents a significant part of this paper (section 3), and a new insight into the nature of FSDP based on the revealed correlations is suggested (section 4).

2. Glass-forming ability: definition and numerical evaluation

The glassy state, as is generally accepted, is obtained when cooling a melt far below its melting point T_m with a final transition into amorphous solid below the glass transition temperature $T_g \sim (\frac{2}{3})T_m$. Obviously, the lower the minimum cooling rate and the more stable this amorphous solid is to further crystallization, the higher the glass-forming ability (GFA) of a substance. Therefore, a number of definitions for GFA, from qualitative to quantitative, exist.

First, one may call 'glass' every amorphous substance that has been prepared by melt cooling. However, in this case there is no difference between, say GeO_2 prepared easily in the form of bulk amorphous material by means of slow cooling of a massive melt, and Ge, which can be prepared as an amorphous solid from the melt only in the form of a thin film obtained by melt sputtering [10], the usual method of obtaining a-Ge being deposition from vapour onto a cooled substrate. To reduce this uncertainty, let us call 'glass' a bulk amorphous solid (1 g and more) that was obtained by relatively slow melt cooling (10^2 K s^{-1} and lower, respectively), thus distinguishing glass-forming substances (or, more strictly, glass-forming melts) from non-glass-forming ones [11].

Secondly, when analysing a glass-forming system (e.g. SiO_2–Na_2O, As–S, etc.), the first task is to determine its glass-forming region, which, first of all, depends on the conditions of melt cooling in a concrete experiment. This region is minimum for slow cooling when a large amount of melt freezes in a furnace, larger when the furnace is blown through with air, and maximum when special quenching into air, water, or other fast cooling agent is employed. Such data may be used for a semiquantitative determination of GFA, as shown in figure 1 (curve 1), where 'glass-forming difficulty' is inverse GFA.

Finally, one may obtain a curve 1 in figure 1 in a quantitative form by means of a special critical cooling rate (CCR) experiment, the CCR value Q_c being defined usually as 'the cooling rate below which detectable crystalline phases are obtained from the melt' [14]. The problem is what amount of crystalline phase is considered as 'detectable'; it varies from crystallization degree $X = 1\%$ (10^{-2}) to $X = 10^{-4}$–10^{-6}. The latter is usual in the cases when experimental crystallization data are extrapolated by means of classical crystallization equations [15] (e.g. curve 2 in figure 1 was obtained just by this method with $X = 10^{-6}$).

It should be noted here that experimental determination of CCR is a highly laborious task. Therefore, there have been only a few investigations carried out in oxide systems (A_2WO_4–WO_3, where A is alkali metal [16], A_2MoO_4–MoO_3 [17], SiO_2–A_2O [18], B_2O_3–Na_2O [19], Ga_2O_3–CaO with impurities [20] and SiO_2–Li_2O with impurities [21]) and in chalcogenide ones (As–Te [22], As_2Se_3–As_2Te_3, As_2Se_3–Tl_2Se, As_2Te_3–Tl_2Te, $GeSe_2$–Tl_2Se and As_2Te_3–Ga_2Te_3 [23], Se–Te [24] and Se–Ge (see curve 1 in figure 1)). In addition,

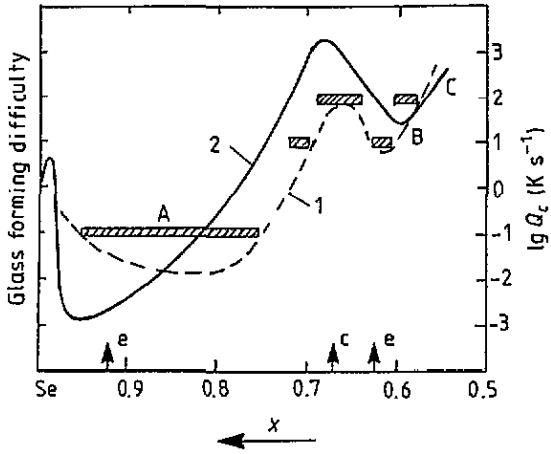

Figure 1. *Glass-forming ability (inverse of* glass-forming difficulty) in the Se_xGe_{1-x} system. Broken curve 1 is a semiquantitative estimation made on the basis of data from [12, figure 2] with A referred to as 'slow cooling', B 'air quenching' and C 'water quenching'. Full curve 2 is experimental CCR after Dembovsky *et al* (cited by [13, p 147]). Letters 'e' and 'c' indicate eutectics and compound ($GeSe_2$) in the Se–Ge phase diagram.

it should have been borne in mind that the *precise* determination of Q_c is impossible since CCR depends on the chosen X ($10^{-2}...10^{-6}$), the experimental procedure, impurities [20, 21] and the extrapolation treatment of crystallization data, if used. Nevertheless, when using one and the same method for a group of substances in which GFA is to be compared, the obtained Q_c values give quite sufficient quantitative information about GFA. In the much more frequent case when such information is absent, we shall use both calculated Q_c data from [15] and [13, (p 145)] and semiquantitative or quantitative evaluations of GFA discussed in this section.

3. First sharp diffraction peak in substances with different glass-forming abilities

3.1. Temperature dependence of first sharp diffraction peak

The critical cooling rate, as a quantitative characteristic of GFA, has to be related to the melting point (T_m), since above T_m an amorphous substance represents a true melt, and below T_m, the lower the temperature, the lower the cooling rate that may be applied without violation of the amorphous state of a substance, which now represents a supercooled melt. Similarly, with the object of quantitative comparison of different substances as concerns FSDP, the data should be reduced to a reference temperature since FSDP, especially its intensity, is temperature-dependent. To illustrate this, a summary of experimental data is presented in figure 2.

It is seen clearly in figure 2 that the FSDP intensity (here in the unified form of structure factor) displays a less or more complex temperature behaviour depending on the substance and the temperature interval investigated and, possibly, on some other factors not so obvious (compare lines 2 and 3 for instance). One may see also that there are no two substances in figure 2 that look like one another, and therefore each case should be considered separately.

For the GeS_2 glass (i.e. bulk amorphous solid existing below T_g, contrary to supercooled liquid existing at $T_g < T < T_m$ or melt at $T > T_m$), there is an *increase* of the FSDP intensity with temperature (see line 1 in figure 2). Remember that in crystals the temperature behaviour of all the diffraction peaks is the opposite: due to increasing thermal motion 'reflections become progressively more diffuse and finally merge with the background' [33, p 146]. Moreover, it follows from the theory that the first peak in the diffraction pattern should decrease most rapidly in accordance with the rapid decrease of the Debye–Waller factor with increasing angle θ [33, p 146]. Thus, the temperature-induced strengthening of

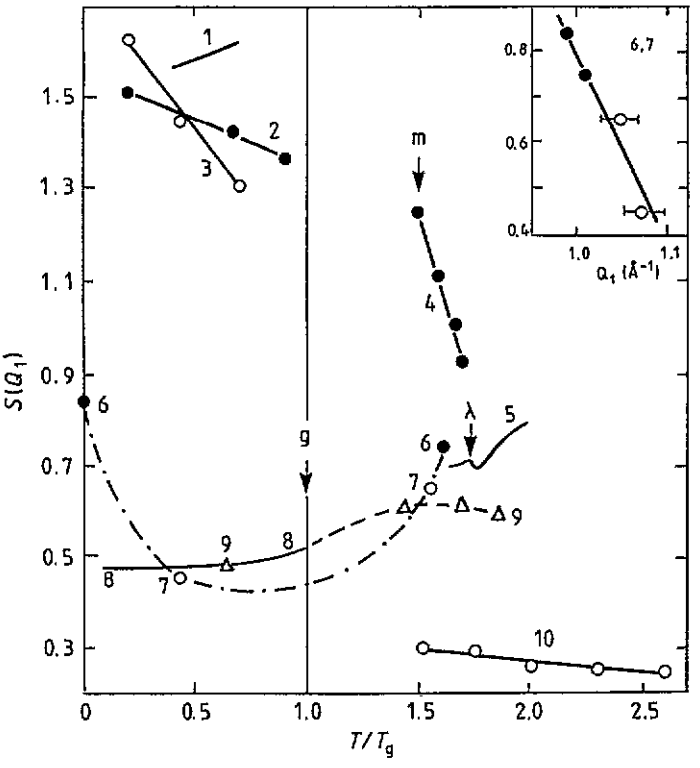

Figure 2. Structure factor at the FSDP maximum as a function of temperature for: 1, GeS_2, [25]; 2, SiO_2 [26]; 3, SiO_2 [27]; 4, KSn [8]; 5, S [28]; 6, $GeSe_2$ [29]; 7, $GeSe_2$ [30]; 8, As_2Se_3 [31]; 9, As_2Se_2 [30]; 10, CCl_4 [32]. Arrows g, m and λ indicate corresponding temperatures (for KSn, T_g is conditionally $2T_m/3$). All the data correspond to neutron diffraction, except 1 and 8 (x-ray). The insert is discussed in the text.

FSDP and thus *ordering* in medium-range order when heating are surprising facts that are not explained sufficiently up to now.

Although the SiO_2 glass demonstrates a 'normal' temperature behaviour, there is no quantitative agreement between the data from different sources (see lines 2 and 3 in figure 2). Moreover, in an early x-ray study [34] there was found to be an *increase* in the FSDP intensity with temperature, namely 450 eu† (300 K) <475 eu (723 K) <530 eu (923 K), i.e. there is an 18% increase when T/T_g varies from 0.20 to 0.62. Note that there is a 5% and 17% *decrease* in structure factor in the same temperature interval for lines 2 and 3 in figure 2, respectively. In order to clear up this discrepancy, the authors of [26] (neutron scattering) have measured especially the x-ray diffraction patterns and found that there is *no* temperature dependence of FSDP intensity in the (0.2–0.9) (T/T_g) interval. The proposed explanation is that neutrons and x-rays differ in their sensitivity to O–O and Si–Si structural correlations [26]. However, the question remains why, when using the same radiation, different quantitative [26, 27] (neutron) or even qualitative [26, 34] (x-ray) results were obtained?

If there were no serious experimental mistakes, one should conclude that the sample prehistory (thermal history, impurities, geometry etc.) may influence not only the $S(Q_1)$ value but also the character of the $S(Q_1)$ temperature dependence. Remember that GFA in the form of CCR was shown to be sensitive to impurities—see Q_c in the Se_xGe_{1-x} system in the low-Ge region (figure 1) and [20, 21]. To clarify the situation, it would be useful to join the CCR and FSDP studies in the framework of a single work dealing with one and the same sample with known prehistory. Unfortunately, those studying FSDP are indifferent to the problem of GFA, at least in the quantitative form of CCR, and vice versa.

† Electron units.

For $GeSe_2$ there are only four points (marked 6 and 7 in figure 2) in a wide temperature interval including both glasses and melts (the characteristic temperatures are $T_g = 673$ K and $T_m = 1013$ K; $T_m/T_g = 1.51$). The fact that these points lie on one line $S(Q_1)$ versus Q_1, which is presented in the insert, makes it possible to consider them as belonging to one and the same group of data, thus uniting them by the chain curve 6–7. If this operation is correct, one may say that $GeSe_2$ demonstrates both *decrease* (in glass) and *increase* (in melt) of the FSDP intensity with temperature.

For As_2Se_3 the data of [30, 31] may be interconnected too (see full curve 8 and triangles 9 in figure 2) in spite of different probes (neutrons [30] and x-rays [31]) and prehistory. Contrary to $GeSe_2$, there is a slight *increase* of FSDP in glass and *decrease* in melt.

In the last three cases, liquid (l) KSn (points 4), l-S (5) and l-CCl_4 (10), one may see examples of both the 'normal' decrease of FSDP intensity with temperature (strong for KSn and rather weak for CCl_4) and the complex behaviour for S whose specific temperature T_λ corresponds to the λ-point where strong structure rebuilding of melt takes place.

Table 1. FSDP versus CCR in (a) glasses and (b) Ge_ySe_{1-y} melts. FSDP intensity is after figure 2 (glasses) and [6] (melts), S_{NN} being partial number–number structure factor that gives the main contribution to FSDP. Q_c without references are from figure 1 (curve 2); in parentheses = estimation; with asterisk = calculated value $S(Q_1)$ for $T/T_g = 0.5$.

(*a*) Glasses			(*b*) Ge_ySe_{1-y} melts			
	$S(Q_1)$	lg [Q_c (K s^{-1})]	y	$S_{NN}(Q_1)$	Q_1 (Å^{-1})	lg [Q_c (K s^{-1})]
GeS_2	1.6	(+2) [25]	0.33	0.78	0.99	+ 3.1
SiO_2	1.4	−2.9* [35]	0.40	0.53	0.98	+ 1.4
As_2Se_3	0.48	−2.0 [23]	0.5	0.23	1.11	(+4)
$GeSe_2$	0.44	+ 3.1	1.0	—	—	+ 7* [13]

Returning to the initial question about the possible relation between FSDP and GFA, we have to admit its absence, even when FSDP is reduced to a reference temperature, say T_g or $T/T_g = 0.5$ (see figure 2 and table 1(*a*)). However, one observation seems to be interesting: all glass-forming melts (5, 9, 10) demonstrate an increase or slight decrease of FSDP intensity with heating, while in non-glass-forming KSn melt the intensity falls rapidly with temperature rise, i.e. the sign and, especially, the velocity of the structure factor change on heating a melt may be critical for glass formation. Of course, to prove this statement, the range of melts under investigation should be widened.

3.2. Concentration dependence of first sharp diffraction peak

One may propose that the correlation between FSDP and GFA will be better when using strong compositional dependence of both. However, as seen in table 1(*b*) this suggestion is not confirmed, at least in the case of Ge_ySe_{1-y} melts. The melts, however, are either poor glass-formers ($y = 0.33$ and 0.40) or non-glass-formers ($y = 0.5$ and 1.0), while melts of good GFA corresponding to compositions $y = 0$–0.20 (see figure 1) have not been investigated [6]. Unfortunately, to my knowledge there is at present no glass-forming system investigated carefully in both the FSDP and GFA respects. Moreover, there are only a few works that permit comparison of FSDP and glass-forming region (GFR) of a system, GFR being a very rough characteristic of GFA (see section 2). Let us consider these works briefly.

The $(GeO_2)_x(Na_2O)_{1-x}$ system whose GFR is $x = 1.0$–0.6 [36] was studied by x-ray diffraction [37]. In the $x = 1.0$–0.7 region under investigation both glasses and glass-forming melts showed FSDP at $Q_1 \sim 1.5$ Å^{-1}, which changed from an individual peak in GeO_2 to a shoulder on the next peak on decreasing x.

The Se_xP_{1-x} system has two GFR: $x = 1$–0.52 and $x = 0.40$–0.33 [38]. (This case is analogous to that shown in figure 1 for Ge–Se system: if we use $Q_c = 10^2$ K s^{-1} as the limiting value for glass formation, then there are two GFR, at $x = 1$–0.72 and $x = 0.63$–0.57.) Contrary to the previous case the strongest FSDP is demonstrated by the compositions arranged at the boundaries of GFR (namely, $x = 0.50$ and $x = 0.40$), while the glass-forming compositions ($x = 1.0$, i.e. pure Se, and $x = 0.95$) do not show an observable FSDP [39].

Melts of the $(ZnCl_2)_x(KCl)_{1-x}$ system whose GFR is $x = 1.0$–0.4 [40] were investigated twice: in [41, p 146] by x-rays for $x = 1.0$, 0.69, 0.54, 0.46, 0.29, 0; and in [42] by neutrons for $x = 1.0$, 0.67, 0.50, 0.33, 0.19, 0.10, 0.05, 0. The data of [41] show a gradual degradation of FSDP on decreasing x. However, by means of numerical data from [42], it reveals a more complex behaviour shown in figure 3, from which it is seen that the most intense FSDP corresponds to the GFR boundary, like in the previous system.

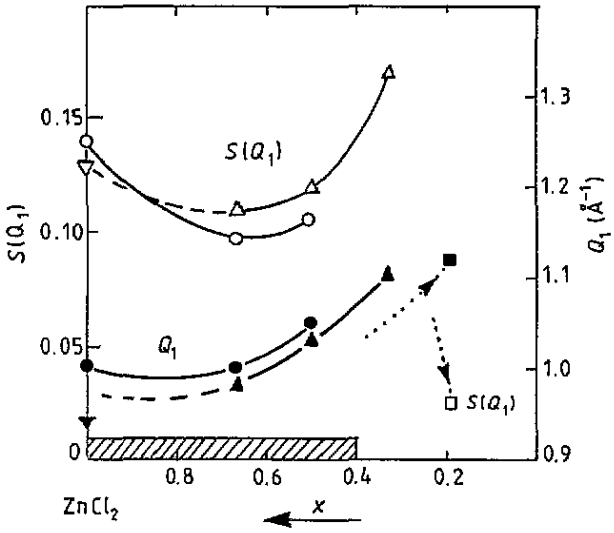

Figure 3. The structure factor and the position of FSDP as a function of composition and temperature of the $(ZnCl_2)_x(KCl)_{1-x}$ melts. Points (after [42]) correspond to 330/340 °C (○, ●), 450 °C (△, ▲), 600 °C (▽, ▼) and 820 °C (□, ■). The glass-forming region (after [40]) is shown by the hatched strip.

In the $(H_3PO_4)_x(H_2O)_{1-x}$ system (glasses are obtained by cooling of aqueous solutions), the GFR is located at $x = 1.0$–0.85, and aqueous solutions under investigation ($x = 0.71$, 0.25, 0.11 and 0.07) show a continuous decrease of FSDP from an individual peak to a shoulder when decreasing x [43] similar to the $(GeO_2)_x(Na_2O)_{1-x}$ system considered above. It is interesting that the last two compositions, which are inside the GFR, demonstrate FSDP as a well defined shoulder on the next peak.

Finally, the Se_xSi_{1-x} system was investigated by Johnson *et al* [44] most thoroughly, and as concerns not only FSDP (intensity, position, halfwidth) but also properties (phase diagram for $x \geqslant 0.4$, molar volume, neutron diffraction, extended x-ray absorption fine structure). Based on the similarity between Si and Ge and that between phase diagrams of the Si–Se and Ge–Se systems, one may suppose the same for their GFA concentration dependence, namely, GFA is expected to increase when moving from $GeSi_2$ to eutectic ($x = 0.92$ for Ge–Se and $x = 0.88$ for Si–Se) in accordance with figure 1. However, as seen in figure 4, the FSDP intensity shows the opposite dependence: when increasing x from

0.67 to 1 (Se) FSDP becomes weaker and weaker and cannot be observed as a separate peak at $x > 0.83$, being practically invisible in pure Se. On the other hand, Se is known to be a better glass-former in comparison with $SiSe_2$, which can be obtained as amorphous solid only by quenching and easily crystallizes on slow cooling of the melt [45].

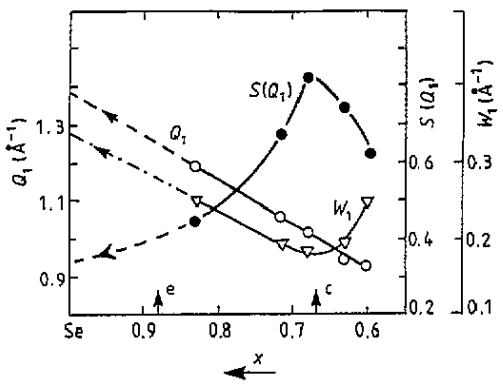

Figure 4. The FSDP parameters as a function of composition for Se_xSi_{1-x} glasses. Points are after [44]. Extrapolation to Se is shown by broken lines and arrows.

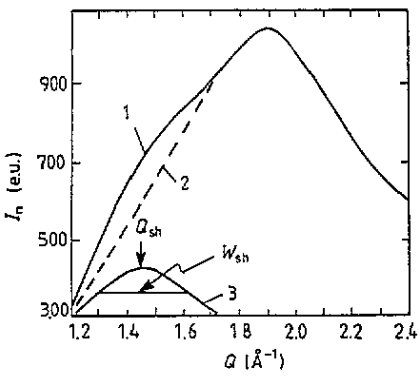

Figure 5. First peak of the normalized experimental intensity in Se glass after [47] (curve 1), and FSDP [3] extracted from it as the difference between curves 1 and 2.

Thus, there is again no clear relation between GFA and FSDP; moreover, the exemplary glass Se seems to be lacking in FSDP, the well established attribute of the glassy state. On the other hand, it was proposed earlier [46] that FSDP in Se glass is hidden behind the first diffuse peak with maximum at $Q \sim 2.0$ Å^{-1}, being a low-Q shoulder on it. When using a detailed peak profile one may extract this shoulder, as is done in figure 5. The obtained parameters ($Q_{sh} = 1.4_5$ Å^{-1} and $W_{sh} = 0.3_5$ Å^{-1}) are close to those obtained by linear extrapolation in figure 4 to $x = 1$ (Se): $Q_1 = 1.38$ Å^{-1} and $W_1 = 0.34$ Å^{-1}. Thus, Se does possess FSDP, like other glasses, but its position is not characteristic for chalcogenide glasses (~ 1.0 Å^{-1}) and just that is the question.

3.3. Scale of medium-range order in glass-forming individuals and systems

The scale of MRO is determined by the equation $\xi = d/r_1$ [9], i.e. it represents equivalent distance for FSDP ($d = 2\pi/Q_1$), considered as the MRO dimension, in units of SRO (short-range order) dimension r_1, the first interatomic distance. The scale of MRO was used earlier for the construction of the ξ–r_1 plot shown in figure 6, in which different groups of amorphous substances (glasses, liquid halides, amorphous metals, APb and ASn melts) are shown to occupy different correlation curves [9]. As to glasses, there are two curves designated G and G′ and an intermediate region between them at $r_1 \sim 2.3$ Å.

Let us consider glasses that were taken in [9] for construction of G and G′ curves from the point of view of their GFA using the following marks for rough estimation of the latter: (+++) very good glass-former, (++) ordinary one and (+) satisfactory one. Curve G (its equation is $\xi = a + b/r_1$ with $a = 1.10$ and $b = 2.27$ Å, its length is from $r_1 = 1.36$ Å to $r_1 = 2.44$ Å): B_2O_3(+++), BeF_2(+++), SiO_2 (++), GeO_2(++), As_2S_3(+++), As_2Se_3(++). Curve G′ ($a = 0$, $b = 6.1$ Å, r_1 from 2.37 Å to 2.60 Å): GeS_2(++), P(+), $Si_{32}S_{68}$(++),

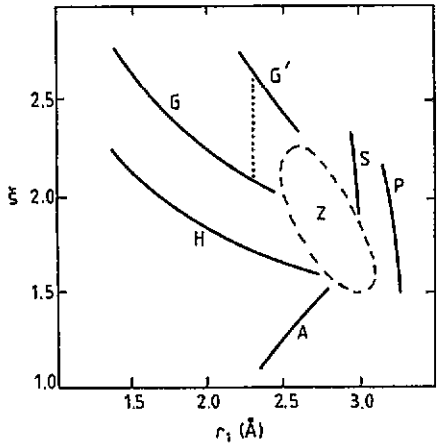

Figure 6. The scale of MRO in amorphous metals (A), glasses (G, G'), liquid halogens (H), ASn melts (S) and APb melts (P); Z is the forbidden zone. Reproduced from [9, figure 2].

$GeSe_2$(+), As(+), $Si_{24}Te_{76}$(+). Intermediate region G–G' ($r_1 \sim 2.3$ Å): $P_{40}Se_{60}$(++), $ZnCl_2$(++). Thus, one may note that very good glasses tend to occupy the G curve while common and poor glass-formers occupy both G and G' curves as well as the intermediate region between them without any natural law.

More distinct correlations arise when one passes from separate glasses to glass-forming system, e.g. Se_xSi_{1-x} shown in figure 7. Homogeneous glasses in this system were obtained and investigated in the work cited above [44] (see also figure 4). In figure 7 numerical data of [44] are drawn on the ξ–r_1 plot, the points $x = 0.88$, 0.94 and 1.0 being obtained with the use of extrapolated Q_1 values given in figure 4 because FSDP is practically invisible in these glasses [44]. It is seen in figure 7 that the glasses under consideration, whose r_1 from 2.294 to 2.359 Å corresponds to the 'unstable' value of ~2.3 Å, fit on one curve, and this curve moves smoothly to higher ξ when decreasing x, crossing the intermediate region between G and G' curves. This fact demonstrates an obvious relation between ξ and composition, but not between ξ and r_1 (e.g. for $r_1 = 2.305$ Å there are two ξ, 2.6 and 2.9), and not between ξ and GFA because the latter should be a much more complex function of x (see figure 1 for example) with an expected maximum at eutectic composition $x \sim 0.88$.

It should be noted also that glasses arranged at the GFA boundary, namely, $x = 0.63$ and 0.60, as well as Se ($x = 1.0$), go out from the limits of correlation curves G and G'. One may observe the same going out in figure 8 for glass-forming melts of the $(ZnCl_2)_x(KCl)_{1-x}$ system represented earlier in figure 3; in this case $r_1 = 2.26$–2.29 Å, however, again corresponds to instability between G and G' curves. In these experiments a new parameter—temperature–is added, and it is seen that the higher the temperature of a melt, the more pronounced deviation from G' is observed.

Finally, to investigate a possible connection between ξ and T let us consider *one* substance at different temperatures, e.g. B_2O_3 shown in figure 9. We see that, as in the previous case, the higher T, the larger ξ and, additionally, their relation changes drastically at T_g: the ξ versus T velocity is rather small in glass ($\partial\xi/\partial T = 5 \times 10^{-5}$) and high in melts ($53 \times 10^{-5}$), both supercooled and true. Note that GFA by definition does not depend on temperature.

Thus, there is no direct connection between scale of MRO and GFA, however, glasses tend to group around definite G and G' curves in the ξ–r_1 plot, and strong deviation from the curves, especially in the high-ξ region, is critical for glass formation.

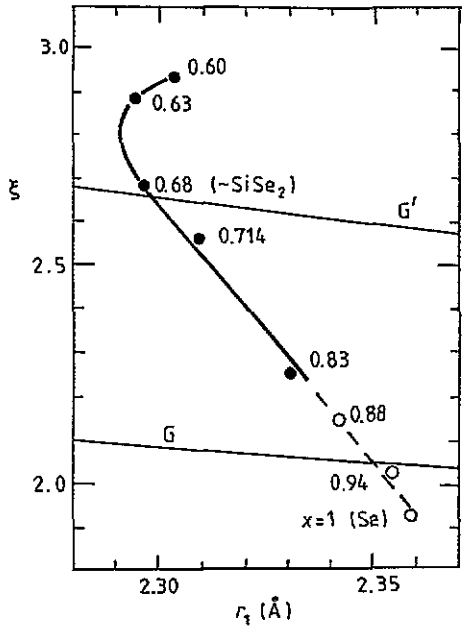

Figure 7. Scale of MRO in Se_xSi_{1-x} glasses. Points correspond to [44]: original data (full circles) and those together with extrapolated Q_1 (open circles). G and G' are fragments of 'glassy' correlation lines.

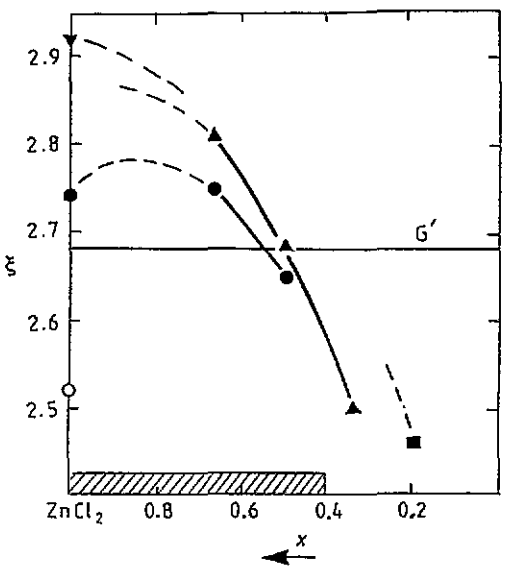

Figure 8. Scale of MRO for $(ZnCl_2)_x(KCl)_{1-x}$ melts at various temperatures: 330/340 °C (●), 450 °C (▲), 600 °C (▼) and 820 °C (■), after data from [42]. Open circle corresponds to $ZnCl_2$ glass [3, table 1]. Hatched strip is GFR.

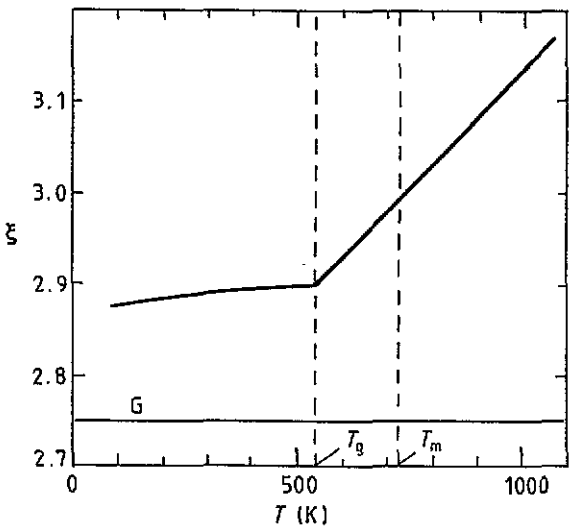

Figure 9. Temperature dependence of the scale of MRO in amorphous B_2O_3 constructed by using d and r_1 from [48]. Line G corresponds to $r_1 = 1.37$ Å (practically constant at 110–1070 K), and G' is absent for this r_1.

4. Discussion

There are many approaches to understanding the origin of FSDP, such as random packing of structural units after Moss and Price [2], chemical ordering of interstitial voids around cation-centred clusters after Elliott [4], oscillating density fluctuations due to local structural units incorporated in an open network structure after Salmon [49], the 'layer' model in which

FSDP is associated with layer-like formations giving Bragg-like reflection (e.g. [31,50]), etc. Below, the modified layer model (MLM) after [51] is tested for conformity with the correlations obtained.

In contrast to the conventional layer model, MLM means that underlying formations are true layers, and their thickness $d = 2\pi/Q_1$ is revealed directly in the diffraction pattern as FSDP. Thus, not interlayer distance but the layer itself gives an elementary Bragg reflection. This means also that FSDP halfwidth, W_1, bears no relation to the length of correlation between a group of layers ('coherence length'), but displays only the roughness of the layer surfaces: the smoother the surfaces, the sharper the FSDP (smaller W_1).

The problem about the nature of such layers was solved in [51]) by means of chemical bond arguments with regards to the parameters of ξ–r_1 correlation curves obtained earlier [9]. It was shown that G and G′ correlation curves characteristic for glasses may be compared with realization of three-centre bonds (TCB) holding the layers, the TCB length $l \geqslant 2r_1$ determining the layer thickness $d \sim l$ as illustrated in figure 10.

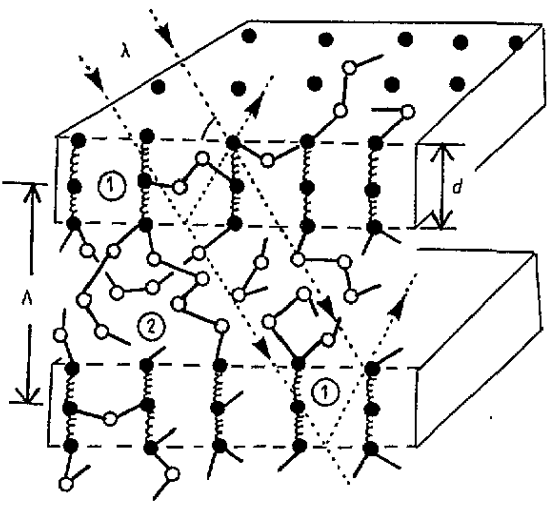

Figure 10. Origin of FSDP as the first-order Bragg reflection from layers (1) divided by amorphous network (2) in a model elementary glass. Here circles are atoms, short lines are covalent bonds (CB) and springs are three-centre bonds (TCB).

From figure 10 it is seen that, while TCB exist only in the limits of the layers, covalent bonds (CB) are present both within (1) and outside (2) them. When considering the layer as an ordered formation, one should conclude that there are two 'types' of covalent network, and network (1) is more ordered in comparison with network (2), which is in fact the famous continuous random network (CRN) after Zachariasen. As experimental justification of two coexisting covalent networks, one may mention the so-called 'defect' peaks on vibrational bands known as D1 and D2 in vitreous silica [52], such peaks being observed also in other glasses (e.g. $GeSe_2$ [53] and As_2S_3 [54]). I think that these rather *sharp* co-peaks originate just from intralayer covalent bonds existing in the ordered quasicrystalline state, while the diffuse main bands are provided by 'normal' vibrations in CRN. Then the change of D1(2) parameters under various external actions described earlier [52, 56, 57] originates from the change of the network (1) topology but not from CRN.

The temperature dependence of the FSDP intensity was shown to have a complex character, both increasing and decreasing with temperature, even for one and the same substance if it is measured over a sufficiently wide temperature interval (see $GeSe_2$ (6, 7), As_2Se_3 (8, 9) and S (5) in figure 2). *A priori* evaluation of temperature dependence for FSDP in the framework of MLM given in table 2 predicts such behaviour because there are

Table 2. Layer parameters as factors influencing FSDP temperature dependence.

Factor	Notation	Change on increasing T	Effect on FSDP		
			Q_1	$S(Q_1)$	W_1
TCB concentration	N_{TCB}	Increase	—	—	—
Layer concentration	N_l	Const or increase	—	Const or increase	—
Layer population	ρ_{TCB}	Increase or const	—	—	—
Roughness of layer	R	Increase (figure 11(b))	—	Decrease	Increase
Thickness of layer	d	Increase (figure 11(b))	Decrease	—	—

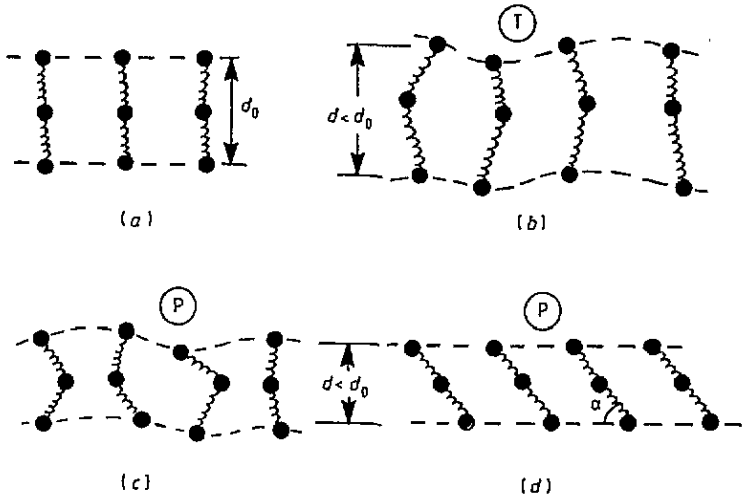

Figure 11. Schemes of TCB layers in ideal (a) and distorted (b,c,d) states; the external distorting factors are indicated in circles.

two oppositely acting factors: the temperature-activated rise in the number of layers and the temperature-stimulated distortion of reflecting surfaces illustrated in figure 11.

Some comments to table 2 are useful for further discussion. Note that TCB themselves do not influence FSDP since the latter arises only when TCB are organized into reflecting layers. Therefore, concentration of TCB is an influential factor only through TCB participation in population of the layer and concentration of layers. If TCB generation is a thermally activated process (in the simplest case $N_{TCB} \sim \exp(-\epsilon/kT)$), there are two limiting ways for the newly generated TCB arrangement: by means of creating new layers without change of their population (N_l increases and ρ_{TCB} = const), and by means of increasing layer population without change of layer concentration (ρ_{TCB} increases and N_l = const). Thus a discontinuous character of the $S(Q_1)$ temperature dependence is possible; however, to reveal such behaviour a more refined experiment is needed.

After [58] the case of N_l = const is realized at T/T_g, and we see for As_2Se_3 (curve 8, 9 in figure 2) that there is a constant or slight increase of $S(Q_1)$ in glass. At higher temperatures the defrozen N_l lifts $S(Q_1)$ initially; however, the opposite action of thermal distortion of the layer surfaces (R increases) gradually depresses this effect and becomes

prevailing at $T/T_g > 1.5$.

For $GeSe_2$ (curve 6–7 in figure 2) the R factor is essential just at $T \ll T_g$, which follows from a strong drop of $S(Q_1)$ when heating from low temperatures. On the other hand, temperature-induced generation of new layers taking place at $T > T_g$ acts in the opposite way, leading ultimately to fast increase of FSDP intensity in the melt.

Thus, the temperature dependence of FSDP should be a complex function, the concrete character of which is determined by the nature of the substance under investigation. Of course, the scheme in table 2 is only a rough approximation, which does not take into account a possible rearrangement of TCB in the layer, which leads to change of its reflecting ability, or transformation of TCB [13] at heating/cooling, etc. Such complications are pointed out from experiment, e.g. the flourish for sulfur at λ-point (see curve 5 in figure 2) may be a signature of layer rebuilding at T_λ, and the impurity influence (compare lines 2 and 3 for SiO_2 in figure 2) indicates that the process of layer formation (like the process of crystallization [20,21]) is sensitive to foreign atoms.

Finally, the difference between non-glass-forming KSn and glass-forming melts, which was emphasized above as the fast decrease of FSDP when heating of the former (figure 2), may be explained in terms of MLM too. After [51] the bonds that form reflecting layers differ in different groups of substances; they are proposed to be the Zintl ion dimers in the case of APb(Sn) melts. It seems likely that heating not only generates new layers but also tends to destroy these ordered formations; then TCB layers in glass-forming melts demonstrate higher thermal resistivity in comparison with the layers held by Zintl ion dimers, which are, therefore, inclined to depolymerization on heating.

The pressure dependence of FSDP may be evaluated *a priori* too. Pressure (i) compresses the layers, (ii) destorys them and (iii) reorients them. Compression is a general effect, so d decreases and Q_1 increases in every case. There are two way of effecting compression shown in figures 11(c) and (d). The first way (c) distorts the layer surfaces and may lead to layer destruction above a critical stress, so W_1 increases and $S(Q_1)$ decreases. The second way (d) does not distort the surfaces and may even smooth them, so W_1 decreases due to R decreasing while $S(Q_1)$ may either decrease due to N_1 decreasing or increase due to R decreasing. However, this is true only up to a critical angle α below which the layers become unstable.

Reorientation of the layers should appear when *uniaxial* (instead of usual hydrostatic) pressure is applied. Since reorientation needs layer mobility in a covalent network, this effect is expected to be more pronounced at $T > T_g$, e.g. at viscous flow. However, in the low-temperature region a slow reorientation due to the stress-stimulated rebuilding of the covalent network (e.g. at plastic flow or glass squeezing) is also possible. The expected result of reorientation is the appearance of *anisotropy* and, as to the FSDP parameters, W_1 increases and $S(Q_1)$ decreases due to dynamical frustrations, which cause partial destruction and distortion of layers.

Let us compare these predictions with experiment. Hydrostatic pressure, in fact, provokes decrease of d (increase of Q_1) in all glasses investigated so far: As_2S_3 [59], As [60], GeS_2 and GeO_2 [61]. The effect is more or less reversible, which means that initially compressed layers can straighten themselves after the pressure is removed. Available data give no possibility to make definite conclusions about the W_1 pressure dependence, but an obvious decrease of the FSDP intensity is observed for As_2S_3, GeS_2 and As. On the other hand, in GeO_2 there is observed constant and, what is more, a slight increasing intensity, up to 10% at $P \rightarrow 3$ GPa, followed by *slight* decrease at further compression [61]. It is interesting that after the pressure is removed the intensity does not increase, like in other glasses, but falls to 70% of the initial value. Hence the pressure-induced inclined layers in

GeO_2 cannot restore their initial state with $\alpha = 90°$ and are destroyed after release. Thus, although compression usually proceeds by the scheme (*c*) in figure 11 the case shown in (*d*) cannot be excluded.

As to anisotropy, it arises under the influence of uniaxial pressure on glass [50]. The interpretation given in the original work at first sight is close to that proposed here. However, it should be emphasized that there is a major difference between the 'layers' considered in [50], etc., and in MLM [51]. In usual layer models there are no alternative bonds characteristic for the amorphous state, and the layers are similar to those existing in the corresponding crystals, e.g. in As_2S_3, which consists of covalent sheets with the distance d between them. The fact that FSDP exists in amorphous substances without a 2D crystal parent needs special justification that weakens these models. In MLM the crystal motif of bonding (1D, 2D, 3D) is of no importance because the layers under consideration are self-sufficient formations based on alternative bonds. This means that in usual layer models pressure influences CRN, while in MLM it influences both CRN (network (2) in figure 10) and the layers (TCB coexisting with network (1)) and just the latter ordered network we observe by means of pressure-induced changes in FSDP.

In contrast to the temperature and pressure dependences of FSDP, the concentration dependence (see figures 3, 4, 7, 8) cannot be predicted by MLM in its present form. However, it is possible to comment on incorporation of foreign atoms (e.g. Si in Se, or K in $ZnCl_2$) in terms of internal pressure and effective heating considered below.

In Se_xSi_{1-x} glasses continuous increase of Q_1 with x (figure 4) points out that incorporating Si atoms causes the layers to burst. Then the Si action may be associated with the increase of intralayer pressure P_1 whose value is determined by

$$\Delta Q_1\big[P_1(\Delta x)\big] = \Delta Q_1\big[P(x_0)\big] \qquad \Delta x = x_0 - x = \text{const}$$

where $P(x_0)$ is the external pressure that should be applied to a given composition (x_0) in order to eliminate the effects of incorporated Si atoms on Q_1 when $x_0 \to x$.

In pure Se an abnormally large (for chalcogenides) $Q_1 \sim 1.4$ Å^{-1} (figure 5) indicates that selenium layers are compressed by surrounding covalent network (2), which leads to the situation shown in figure 11(*c*) with $P = P_z$. Thus, incorporating Si atoms, which increases P_1, continuously straighten the initially distorted layers, which is reflected in figure 7 as increase of ξ which enters into the 'normal' G–G′ region when $x < 0.9$; this transition corresponds to the change from figure 11(*c*) to 11(*a*). Then the composition of $x \sim 0.68$, where FSDP possesses maximum intensity and minimum halfwidth (figure 4), may be considered as corresponding to the case $P_1 = P_2$ when total stress on TCB is absent ($d = d_0$). On further incorporation of Si atoms P_1 becomes larger than P_2, and the layers begin to stretch ($d > d_0$) with subsequent distortion of reflecting surfaces; this corresponds to change from (*a*) to (*b*) in figure 11. For $x < 0.60$ intralayer stress due to P_1 is so high that TCB and layers themselves begin to be destroyed, which leads to drastic decrease of GFA and going out from GFR.

The data for glass-forming melts $(ZnCl_2)_x(KCl)_{1-x}$ (figures 3, 8) give an opportunity to discuss effective heating, ΔT^*, due to the second component of a system. For instance, in order to keep ξ in the alloy with $x = 0.6$ and $T = 340$ °C (figure 8) when changing its composition from, say, 0.60 to 0.53, we should heat it at the same time from 340 °C to 450 °C. Therefore, incorporation of corresponding amount of KCl may be described as heating of initial melt by $\Delta T^* = 110$ °C. From figure 8 it is seen that, the lower x, the larger is ΔT^* for the same Δx, so one may interpret the going out from GFR at $x < 0.4$ as the advance of effective superheating $(\partial T^*/\partial x) > (\partial T^*/\partial x)_{\text{crit.}}$. The compositionally 'superheated' melts seem to lose the ability for glass formation.

Thus, MLM may predict, explain and, at least, describe the experimentally observed features of FSDP including correlations obtained in this work. To my knowledge, such a detailed interpretation has not been achieved in the framework of other models of FSDP. However, MLM like other models says nothing about the origin of MRO. Actually, each real-space interpretation of FSDP operates with more or less definite structural units (see [1–4, 49, 50] and references therein), and MLM is not an exception, the units being layers populated with alternative bonds. But the questions are why such units (e.g. soft cation-centred clusters after Elliott [24], etc.) are realized in some amorphous substances and not in others, what is the mode of their formation/destruction, and so on. Therefore we must go beyond the limits of the above models and try to reveal the *origin* of underlying structural units besides their description. For MLM such a basis is given by the synergetic model of FSDP after [58].

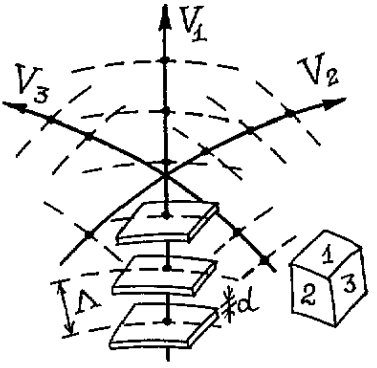

Figure 12. Three coexisting bond waves giving anisotropic cellulate structure with elementary cell of Λ dimension. Vectors V_i are wave velocities. Both Λ and V are temperature dependent.

The synergetic model considers FSDP and corresponding MRO as a result of inherent *bond instability* in the form of a *bond wave*; the former means coexistence and exchange of main and alternative bonds, and the latter means spatiotemporal correlation of the bond exchange acts. Corresponding wavefronts are populated with alternative bonds while the medium consists of main bonds only. Thus one may consider figure 10 as an illustration of a TCB wave in which two adjacent wavefronts are shown. Interlayer distance Λ is actually the wavelength, and the general consequence of the synergetic model is that there exists not only MRO but also LRO (long-range order) of period Λ. This LRO, however, does not exclude isotropy usually observed in amorphous state (figure 12).

The bond wave is proposed to be travelling above T_g and frozen in brittle glass, where wavefronts/layers are immovable. Since wavefronts are occupied by alternative bonds, the local properties differ from average ones, so in glasses, where alternative bonds are 'soft' TCB with $l \geqslant 2r_1$ [13], the layers are softer and less dense formations in comparison with interlayer covalent network(2) (see figure 10). Thus, a travelling bond wave may be compared with an acoustic wave or periodic density fluctuations in the structure. It should be noted that Salmon [49] emphasized that (i) FSDP confers a marked oscillatory character of periodicity $2\pi/k_1$ ($k_1 \equiv Q_1$), and (ii) underlying 'structural units, which give rise to the density fluctuations on the IRO (≡ MRO) scale, exist as stable entities for a time scale $\tau \gg 5 \times 10^{-12}$ s'. In the framework of MLM and synergetic model this means that (i) there exist also higher-order Bragg reflections ($n = 2, 3, \ldots$) besides FSDP ($n = 1$), and (ii) the

frequency of bond wave, which increases with temperature, should not be very high—an obvious demand to prevent disruption into chaotic bond exchange instead of bond wave.

5. Conclusions

The analysis of available experimental data on FSDP as functions of temperature, pressure and composition shows that there is no direct relation between FSDP and GFA. However, the FSDP parameters are sensitive to internal processes in glasses/melts and react on the going on from the glass-forming region. The correlations obtained should be taken into account by any model that pretends to explain the FSDP origin, and the modified layer model was tested successfully in this respect. On the other hand, any model that operates with structural units (clusters, layers, etc.) should explain not only what these units are but also whence they are. Here the synergetic model, which treats FSDP as a result of self-organization of chemical bonds in the form of a bond wave, was used. Each amorphous substance possessing conditions for such self-organization, i.e. bond instability and spatiotemporal correlation of bond exchange, possesses at the same time FSDP, which is, therefore, a much more general phenomenon than glass formation. The specificity of glass-formers consists in enhanced stability of bond waves at cooling below the melting point; then the indirect relation between FSDP and GFA is not surprising and needs a deeper investigation.

Acknowledgment

This work was supported by Russian Foundation for Fundamental Research (Grant No 93-03-456).

References

[1] Phillips J 1981 *J. Non-Cryst. Solids* **43** 37
[2] Moss S C and Price D L 1985 *Physics of Disordered Materials* ed D Adler, H Fritzsche and S R Ovshinsky (New York: Plenum) p 77
[3] Wright A C, Hulme R A, Grimley D I, Sinclair R N, Martin S W, Price D L and Galeener F L 1991 *J. Non-Cryst. Solids* **129** 213
[4] Elliott S R 1992 *J. Phys.: Condens. Matter* **4** 7661
[5] Cervinka L and Hruby A 1982 *J. Non-Cryst. Solids* **48** 231
[6] Salmon P S and Liu J 1994 *J. Phys.: Condens. Matter* **6** 1449
[7] Reijers H T J, Saboungi M-L, Price D L, Richardson J W and Volin K J 1989 *Phys. Rev.* B **40** 6018
[8] Reijers H T J, Saboungi M-L and Price D L 1990 *Phys. Rev.* B **41** 5661
[9] Chechetkina E A 1993 *J. Phys.: Condens. Matter* **5** L527
[10] Vucic Z, Etlinger B and Kunstel D 1976 *J. Non-Cryst. Solids* **20** 451
[11] Dembovsky S A and Chechetkina E A 1982 *Mater. Res. Bull.* **17** 1531
[12] Azoulay R, Thibierge H and Brenac A 1975 *J. Non-Cryst. Solids* **18** 33
[13] Dembovsky S A and Chechetkina E A 1990 *Glass Formation* (Moscow: Nauka)
[14] Sargeant P T and Roy R 1968 *Mater. Res. Bull.* **3** 265
[15] Uhlmann D R 1972 *J. Non-Cryst. Solids* **7** 337; 1981 *J. Non-Cryst. Solids* **38/39** 693
[16] Gelsing R T H, Stein H N and Stevels J M 1966 *Phys. Chem. Glasses* **7** 185
[17] van der Wielen J C, Stein H N and Stevels J M 1968 *J. Non-Cryst. Solids* **1** 18
[18] Havermans A C J, Stein H N and Stevels J M 1970 *J. Non-Cryst. Solids* **5** 66
[19] Baeten M H C, Stein H N and Stevels J M 1972 *Silicates Industriels* **37** 33
[20] Whichard G and Day D E 1984 *J. Non-Cryst. Solids* **66** 477
[21] Huang W, Ray C S and Day D E 1986 *J. Non-Cryst. Solids* **86** 204
[22] Mikhailov M D and Tveryanovich A S 1980 *Fiz. Khim. Stekla* **6** 543
[23] Mikhailov M D and Tveryanovich A S 1986 *Fiz. Khim. Stekla* **12** 274
[24] Dembovsky S A, Ilizarov L M and Khar'kovsky A Yu 1986 *Mater. Res. Bull.* **21** 1277

[25] Lin C, Busse L E, Nagel S R and Faber J 1984 *Phys. Rev.* B **29** 5060
[26] Susman S, Volin K J, Montague D G and Price D L 1991 *Phys. Rev.* B **43** 11076
[27] Graneli B and Dahlborg U 1989 *J. Non-Cryst. Solids* **109** 295
[28] Winter R, Bodensteiner T, Szornel C and Egelstaff P A 1988 *J. Non-Cryst. Solids* **106** 100
[29] Susman S, Price D L, Volin K J, Dejus R J and Montague D G 1988 *J. Non-Cryst. Solids* **106** 26
[30] Uemura O, Sagara Y, Muno D and Satow T 1978 *J. Non-Cryst. Solids* **30** 155
[31] Busse L E and Nagel S R 1981 *Phys. Rev. Lett.* **47** 1848
[32] Misawa M 1989 *J. Chem. Phys.* **91** 5648
[33] Klug H P and Alexander L E 1974 *X-ray Diffraction Procedures for Polycrystalline and Amorphous Materials* (New York: Wiley)
[34] Soklakov A I and Nechaeva V V 1967 *Fiz. Tverd. Tela* **9** 921
[35] Ruckenstein E and Ihm S K 1976 *J. Chem. Soc., Faraday Trans. I* **72** 764
[36] Ota R and Kanugi M 1977 *Proc. XI Int. Congr. Glasses (Prague)* p 249
[37] Kamiya K, Yoko T, Itoh Y and Sakka S 1986 *J. Non-Cryst. Solids* **79** 285
[38] Kim E I, Chernov A P, Dembovsky S A and Borisova Z U 1976 *Neorg. Mater.* **12** 1021
[39] Price D L, Misawa M, Susman S, Morrison T I, Shenoy G K and Grimsditch M 1984 *J. Non-Cryst. Solids* **66** 443
[40] Jiang Z, Hu X and Hou L 1986 *J. Non-Cryst. Solids* **80** 543
[41] Vatolin N A and Pastukhov E A 1980 *Diffraction Study of High-Temperature Melts* (Moscos: Nauka)
[42] Allen D A, Howe R A, Wood N D and Howells W S 1992 *J. Phys.: Condens. Matter* **4** 1407
[43] Ivanov A A, Kirilenko I A, Kuznetzov V V, Kravchuk K G and Trostin V N 1990 *Dokl. Akad. Nauk SSSR* **331** 919
[44] Johnson R W, Price D L, Susman S, Arai M, Morrison T I and Shenoy G K 1986 *J. Non-Cryst. Solids* **83** 251
[45] Berezhnoi A S 1958 *Silicon and Its Binary Systems* (Kiev: Urk. Akad. Nauk)
[46] Chechetkina E A 1991 *J. Non-Cryst. Solids* **128** 30
[47] Wei W, Corb B W and Averbach B L 1982 *J. Non-Cryst. Solids* **53** 19
[48] Misawa M 1990 *J. Non-Cryst. Solids* **122** 33
[49] Salmon P S 1994 *Proc. R. Soc.* A **445** 351
[50] Tanaka K 1990 *J. Non-Cryst. Solids* **119** 254
[51] Chechetkina E A 1994 *Solid State Commun.* **91** 101
[52] Walrafen G E and Hokmabadi M S 1986 *Structure and Bonding in Noncrystalline Solids* ed G E Walrafen and A G Revesz (New York: Plenum) p 185
[53] Bridenbaugh P M, Espinosa G P, Griffiths J E, Phillips J C and Remeika J P 1979 *Phys. Rev.* B **20** 4140
[54] Knight D S, Mecholsky J J and White W B 1987 *J. Am. Ceram. Soc.* **70** 561
[55] Seifert F A, Mysen B O and Virgo D 1983 *Phys. Chem. Glasses* **24** 141
[56] Galeener F L 1985 *J. Non-Cryst. Solids* **71** 373
[57] Krol D M, Lyons K B, Brawer S A and Kurkjian C R 1986 *Phys. Rev.* B **33** 4196
[58] Chechetkina E A 1993 *Solid State Commun.* **87** 171
[59] Tsutsu H, Tamura K and Endo H 1984 *Solid State Commun.* **52** 877
[60] Tanaka K 1988 *Phil. Mag.* B **57** 473
[61] Tanaka K 1988 *Phil. Mag. Lett.* **57** 183